## **Elasticity of Semiflexible Biopolymer Networks**

F. C. MacKintosh, <sup>1,2</sup> J. Käs, <sup>1,3</sup> and P. A. Janmey <sup>1,3</sup>

<sup>1</sup>Institute for Theoretical Physics, University of California, Santa Barbara, California 93106-4030

<sup>2</sup>Department of Physics, University of Michigan, Ann Arbor, Michigan 48109-1120

<sup>3</sup>Division of Experimental Medicine, Brigham and Women's Hospital, Harvard Medical School, Boston, Massachusetts 02115

(Received 10 July 1995)

We develop a model for cross-linked gels and sterically entangled solutions of semiflexible biopolymers such as F-actin. Such networks play a crucial structural role in the cytoskeleton of cells. We show that the rheologic properties of these networks can result from nonclassical rubber elasticity. This model can explain a number of elastic properties of such networks *in vitro*, including the concentration dependence of the storage modulus and yield strain.

PACS numbers: 61.25.Hq, 82.70.Gg, 83.80.Lz,

A variety of semiflexible biopolymers and protein filaments affect cell structure and function. The most prevalent of these in eucaryotic cells is actin, which forms the cytoskeletal rim [1,2]. This actin cortex is a polymer gel that provides mechanical stability to cells, and plays a key role in cell motion. Networks of actin and other protein filaments in vitro have been the subject of considerable recent interest [1-7], not only because of their structural role in cells, but also because of the unusual viscoelastic properties of these networks. Such protein filaments as actin are novel in that they form viscoelastic networks, in which  $a \ll \xi \lesssim \ell_p$ , where a is the size of a monomer,  $\xi$ is the characteristic "mesh" size of the network, and  $\ell_p$  is the persistence length of a chain. In the case of actin,  $\xi$ and  $\ell_p$  are of order 1  $\mu$ m, as illustrated in Fig. 1. This, for instance, has permitted direct visualization of polymer dynamics such as reptation [8,9] by optical microscopy [7]. Insight into the control of viscoelasticity in networks of both natural and synthetic semiflexible polymers in this intermediate regime is also important for the design of biocompatible materials. For instance, aqueous gels of stiff protein filaments or biocompatible polymers have both structural and pharmaceutical applications. However, neither models of flexible-chain solutions nor models of rigid-rod networks [8,9] are directly applicable to such systems. Here we report a model for the elasticity of semiflexible polymer networks that can account for many of the observed properties of such networks in vitro.

Concentrated solutions and gels of flexible polymers are characterized by entanglement points where polymer strands cross and loop around each other. Permanent networks or gels can be formed by chemical crosslinks that determine the average distance between points along a given chain that are effectively constrained by the surrounding network. For a solution, on the other hand, the viscoelastic properties depend on transient entanglements of an individual chain with its neighbors [8,9]. Despite the transient nature of these entanglements, over intermediate time scales of interest, the effect is much the same as that of chemical cross-links, although

the effective degree of entanglement or the average length  $L_e$  between entanglements is more subtle. This intermediate regime is the "rubber plateau," for which the solution behaves as an elastic solid. It is this regime that we address below.

F-actin at concentrations between  $36 \mu g/ml$  and 2 mg/ml forms viscoelastic solutions without permanent cross-links, but the arrangement of filaments is different from that of flexible polymers. Solutions of actin filaments in vitro exhibit a polydisperse length distribution of about 2 to 70  $\mu m$  in length, with a mean length of  $22 \mu m$  [10]. On the scale of the mesh size  $\xi < \ell_p$ , chains cannot form loops and knots [11–13] since their persistence length is substantially longer. Therefore, the structure of a molecular constraint between two actin

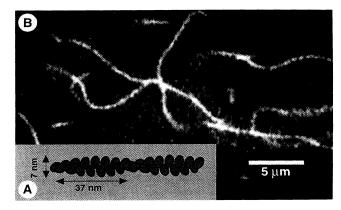


FIG. 1. Entangled network of semiflexible actin filaments. (A) In physiological conditions, individual monomeric actin proteins (G-actin) polymerize to form double-stranded helical filaments known as F-actin. These filaments exhibit a polydisperse length distribution of up to 70  $\mu$ m in length. The persistence length of these filaments is of order 2  $\mu$ m. (B) A dense solution (1.0 mg/ml) of actin filaments, approximately 0.03% of which have been labeled with rhodamine-phalloidin in order to visualize them by fluorescence microscopy. The average distance  $\xi$  between chains in this figure is approximately 0.3  $\mu$ m. Note the nearly straight conformation of the filaments on this scale.

filaments will differ from that of two entangled random coils, and perhaps the term entanglement is not entirely appropriate in this context. Nevertheless, we shall retain the term entanglement length and the corresponding symbol  $L_e$  in analogy with flexible systems, and to emphasize that the relevant length for elastically active contacts is distinct from the average difference between overlapping polymers, or the mesh size.

Many of the properties that are apparently important for the function of the actin cortex are essentially different from those of gels and concentrated solutions of flexible polymer chains. Although some viscoelastic properties of actin and other biopolymer networks resemble those of high molecular weight solutions of flexible polymer chains, the rubber plateau regime exhibits novel behavior. Actin solutions, for instance, exhibit relatively high plateau moduli, of order 100 Pa or higher for actin monomer concentrations of order 1 mg/ml (i.e., for volume fractions of order 0.1%) [6]. Similarly high shear moduli are also measured for the biopolymer fibrin. For comparison, high molecular weight polystyrene solutions at higher concentrations of order 1% exhibit moduli of only about 1 Pa [14]. The plateau modulus of actin networks also exhibits significant strain hardening for modest strains. A rather small linear regime is observed; e.g., in many cases they have a threshold strain as low as (5-10)%, beyond which they lose their mechanical integrity. In the case of actin, this maximal strain also weakly decreases with increasing actin concentration [15]. As we show, this is a direct consequence of the intrinsic bending rigidity of biopolymers such as actin, and is direct evidence of the inapplicability of the freely jointed chain model for the concentrations of interest [16,17].

We propose a mechanism for elasticity in these networks that is still entropic in origin, but which can account for the rather large moduli. We shall focus primarily on actin networks, although our model is applicable to other semiflexible polymers at intermediate concentrations. We develop a model for densely crosslinked actin gels and entangled solutions, in which the elastic properties arise from chains that are very nearly straight between entanglements, as illustrated in Fig. 1. As we shall focus on the elastic rubber plateau modulus, we shall not distinguish between cross-linked gels and entangled solutions, except insofar as the entanglement lengths may differ. We show that for an entangled solution, the plateau modulus scales with concentration  $c_A$  as  $G' \sim c_A^{11/5}$ . As shown in Fig. 2 this is consistent with the measurements to date of the concentration dependence of G' in the range of 0.3-2.0 mg/ml [4]. For densely cross-linked gels, however, a somewhat stronger,  $G' \sim c_A^{5/2}$ , dependence is predicted.

In our model for the linear elasticity in the plateau regime, we consider an ensemble of chain segments of length  $L_e$  (either between cross-links or entanglement

points), which are embedded in a continuous medium that undergoes a uniform shear deformation characterized by angle  $\theta$ . This assumption of a simple, affine deformation should be valid only to describe the linear response of the network. The elastic response of the network results from the tension in such chain segments as a function of the extension,  $L-L_0$ , where  $L_0$  is the relaxed length. When a semiflexible chain segment is stretched by a tension  $\tau$ , the energy per unit length of the chain depends on two effects: the bending of the chain, and the work of contracting against the applied tension. The energy per unit length can be written [19]

$$H = \frac{1}{2}\kappa(\nabla^2 u)^2 + \frac{1}{2}\tau(\nabla u)^2, \tag{1}$$

where  $\kappa$  is the chain bending modulus, and u(x) describes the (transverse) deviation of the chain away from a straight conformation along the x axis.  $\kappa$  is related to the persistence length of the chain  $\ell_p$  (the length over which the chain appears straight in the presence of thermal undulations) by  $\ell_p \simeq \kappa/kT$ . We let  $L_{\infty}$  denote the full contour length of the chain (i.e., for  $\kappa = \infty$  or  $\tau = \infty$ ). We neglect the possibility of "internal" stretching of the chain; i.e., the chain is assumed to have no longitudinal compliance. Thus, for fixed contour length,  $L_{\infty} - L \simeq \frac{1}{2} \int dx \, (\nabla u)^2$ . At a given temperature and for a given tension  $\tau$ , the transverse thermal fluctuations of u determine the equilibrium length L. The chain conformation can be described by the Fourier series  $u(x) = \sum_{q} u_q \sin(qx)$ , where we include wave vectors  $q = \pi/L, 2\pi/L, \dots$  consistent with fixed ends of the chain segment. For the harmonic energy of Eq. (1), the mean square amplitudes  $\langle u_a^2 \rangle$  can be calculated

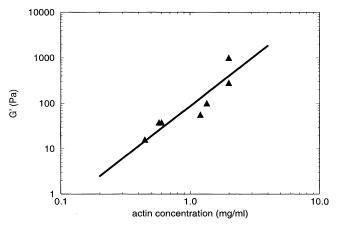


FIG. 2. The plateau modulus G' of actin networks as a function of concentration in mg/ml [4]. The predicted scaling for entangled networks, from Eq. (8), is shown. In this case,  $G' \sim c_A^{11/5}$ . A nematic phase of actin filaments has been shown to form above a concentration of approximately 2 mg/ml [18]. Our model is valid for the entangled isotropic regime [11]  $(kT/\kappa)^2/a < c_A < kT/(\kappa a^2)$ .

from the equipartition theorem, with the result that

$$L_{\infty} - L \simeq kT \sum_{q} \frac{1}{\kappa q^2 + \tau}, \qquad (2)$$

where we have included both transverse polarizations of u. To linear order in applied tension  $\tau$ , the average end-to-end distance of the chain segment is  $L \simeq L_{\infty} - kTL^2/(6\kappa) + kTL^4/(90\kappa^2)\tau$ . The second term represents the equilibrium contraction of the end-to-end distance at finite temperature. The last term gives the linear relationship between the applied tension and extension  $\delta L$  of the chain segment beyond its relaxed length. For small deformations, the restoring force for either extension or compression is given by [20]

$$\tau \sim \frac{\kappa^2}{kTI^4} \, \delta L \,. \tag{3}$$

The above results for the behavior of individual chains can be used to estimate first the maximum shear strain  $\theta_{\rm max}$  that a network can withstand. This will, in general, decrease with increasing concentration, since the entanglement length will then decrease. This means that the fraction of the excess chain length in the form of thermal undulations decreases, and hence there is less chain available to "pull out" under the applied stress. More precisely, the relative extension of a segment of length  $L_e$  between entanglements is proportional to the strain  $\theta$ :  $\delta L \sim \theta L_e$ . Considering the total excess length  $L_{\infty} - L_0$ above, the maximum strain for chain segments of length  $L_e$  is given by  $\theta_{\rm max} \sim kTL_e/\kappa$ . Thus, the maximum strain is predicted to depend linearly on Le. Furthermore, this maximal strain decreases with increasing chain stiffness (for the same entanglement length  $L_e$ ). This is consistent with the observation that the yield strain does indeed increase with increasing flexibility of the network: networks of ADP actin, ATP actin, and vimentin show such a trend [17].

For the modulus G' we use the relation above for the tension on an individual chain segment as a function of the shear strain in the linear regime. For a network, we consider a chain segment of length  $L_e$  that is deformed by an amount given by  $\delta L \sim \theta L_e$ . Of course, the deformation depends on the orientation of the segment. For small strain  $\theta$ , the restoring force under both extension and compression [Eq. (3)] contributes to the linear elasticity of a network. Solutions and gels are characterized by a mesh size  $\xi$  that describes the average spacing between chains or the size of voids between filaments. Along a plane parallel to the shear, there are  $1/\xi^2$  chains per unit area [9]. The stress  $\sigma$  is therefore given by  $\sigma \sim \kappa^2/(kT\xi^2L_e^3)\theta$  in the linear regime. Thus the modulus scales as

$$G' \sim \frac{\kappa^2}{kT} \, \xi^{-2} L_e^{-3} \,.$$
 (4)

This is in contrast with the behavior of gels and networks of flexible chains, for which  $G' \sim kT/\xi^3$  [8].

Both the entanglement length  $L_e$  and the mesh size  $\xi$  decrease with increasing concentration of chains, although, unlike concentrated solutions of flexible chains, the scaling of these quantities with concentration need not be the same when  $L_e \gtrsim \xi$  [21]. The characteristic mesh size  $\xi$  for a network of stiff chains is given by  $\xi \sim 1/\sqrt{ac_A}$ , where  $c_A$  is the concentration of actin monomers of size a [22]. This is valid when the persistence length of the chains is longer than the mesh size  $\xi$ . For a densely cross-linked gel,  $\xi$  is also the typical distance between cross-links, and therefore entanglement points;  $L_e \simeq \xi$ . In this case,

$$\theta_{\rm max} \sim \frac{kT\xi}{\kappa} \sim \frac{kT}{\kappa} (ac_A)^{-1/2}$$
 (5)

and

$$G' \sim \frac{\kappa^2}{kT} \, \xi^{-5} \sim \frac{\kappa^2}{kT} \, (ac_A)^{5/2}.$$
 (6)

The precise dependence of the entanglement length on concentration in a solution of semiflexible chains is less obvious than for flexible systems. We expect that  $L_e$  may become substantially larger than  $\xi$  for  $\xi \lesssim$  $\ell_p$ , since the transverse fluctuations of a semiflexible chain are greatly reduced over distances comparable to or smaller than the persistence length of the chain. We assume that the scaling of this entanglement length is the same as that of the typical distance between binary collisions between chains in solution. This length can be obtained in the following way [11]. From the above energy in Eq. (1), the transverse fluctuations at temperature T of a chain confined (entangled) at one end grow as  $\langle L_{\perp}^2 \rangle \sim kTL^3/\kappa$ , where L is the distance from the entanglement. Thus, the fluctuating chain segments of length  $L_e$  between entanglements occupy a volume  $L_e \langle L_\perp^2 \rangle \sim kT L_e^4 / \kappa$ . For a given concentration  $c_A$ , the probability of an intersection with another chain is of order unity for  $L_e \sim (\kappa/kT)^{1/5} (ac_A)^{-2/5}$ , which becomes larger than  $\xi$  for  $\xi \ll \ell_p$ . Thus

$$\theta_{\text{max}} \sim (kT/\kappa)^{4/5} (ac_A)^{-2/5}$$
 (7)

and

$$G' \sim \kappa (\kappa/kT)^{2/5} (ac_A)^{11/5}$$
. (8)

This model provides a consistent framework with which to understand the macroscopic viscoelasticity of chemically cross-linked and sterically entangled biopolymer solutions. Based on the semiflexible nature of several biopolymers, including F-actin, the model can explain both the large storage moduli as well as the observed strain hardening of networks at moderate to low strains [23], a feature in contrast with the behavior of flexible polymer networks. For instance, at equal volume fractions, vimentin filaments, which are approximately an order of magnitude less stiff than F-actin, form solutions

with smaller shear moduli than F-actin, although vimentin solutions can withstand approximately 10 times larger strains than F-actin before rupturing. Experimental observations of shear moduli and yield strain for varying actin concentration, as well as for modest changes in F-actin stiffness induced by binding of different nucleotides, are also in support of this model.

This model makes several additional predictions that can be tested experimentally. First, as indicated above, for densely cross-linked gels,  $G' \sim \kappa^2$ . Since it is now possible to measure  $\kappa$  directly for actin and some other biopolymers by video microscopy [17], and there are a number of actin binding proteins and metabolites that can alter filament stiffness under conditions where filament length is held constant, the viscoelastic parameters can be directly measured as a function of  $\kappa$ . Furthermore, the scaling behavior of entangled solutions and cross-linked gels as a function of concentration are predicted to differ. A third prediction is that the viscoelasticity of relatively dilute filament networks will be extremely sensitive to filament length even if the average filament length is much greater than the mesh size, and this dependence will be greatest for the stiffest polymers. This is because for semiflexible filaments the entanglement length required for effects on elasticity can be much greater than the mesh size [12,13], and this difference depends on  $\kappa$ . Therefore, subtle changes in filament length can have large effects on viscoelasticity even when all filaments exhibit significant overlap. This feature may be one of the reasons the cytoskeletal actin filaments in cells are under the tight control of proteins that regulate their length.

The authors wish to thank A. Maggs, E. Sackmann, and C. Schmidt for helpful comments. This work was supported in part by NSF Grant No. PHY94-07194. F. C. M. was funded by NSF Grant No. DMR 92-57544 and by the Petroleum Research Fund. J. K. was funded by a Forschungsstipendium of the DFG. J. K. and P. A. J. were funded by NIH Grant No. AR38910.

- [1] E. L. Elson, Annu. Rev. Biophys. Chem. **17**, 397–430 (1988).
- [2] T. Stossel, Science 260, 1086 (1993).
- P. A. Janmey *et al.*, J. Biol. Chem. **261**, 8357 (1986);
   P. A. Janmey, S. Hvidt, J. Lamb, and T. P. Stossel, Nature (London) **345**, 89 (1990).
- [4] P. A. Janmey et al., J. Cell Biol. 113, 155 (1991).
- [5] J. Newman et al., Biophys. J. 64, 1559 (1993);D. Wachsstock, W. Schwarz, and T. Pollard, Biophys. J.

- **66**, 205 (1994); J. Haskell *et al.*, Biophys. J. **66**, A196 (1994).
- [6] P. A. Janmey et al., J. Biol. Chem. 269, 32503 (1994).
- [7] J. Käs, H. Strey, and E. Sackmann, Nature (London) 368, 226 (1994).
- [8] P.G. de Gennes, Scaling Concepts in Polymers Physics (Cornell, Ithaca, 1979)..
- [9] M. Doi and S.F. Edwards, *Theory of Polymer Dynamics* (Oxford University Press, New York, 1986).
- [10] S. Kaufmann, J. Käs, W. H. Goldmann, E. Sackmann, and G. Isenberg, FEBS Lett. 314, 203 (1992).
- [11] A. N. Semenov, J. Chem. Soc. Faraday Trans. 2 82, 317 (1986).
- [12] H. Isambert and A. C. Maggs (to be published).
- [13] A lower plateau modulus with a weaker concentration dependence  $(G' \sim c_A^{1.4})$  is predicted in Ref. [12] for lower concentrations. Here, we have focused on a limit valid for either high concentration or high molecular weight.
- [14] M. Adam and M. Delsanti, J. Phys. (Paris) 44, 1185 (1985).
- [15] P. A. Janmey et al., Biochem. 27, 8218 (1988).
- [16] P. A. Janmey et al., Nature (London) 347, 95 (1990).
- [17] J. Käs, L.E. Laham, D.K. Finger, and P.A. Janmey, Mol. Biol. Cell 5, 157a (1994).
- [18] R. Furukawa, R. Kundra, and M. Fechheimer, Biochem. **32**, 12 346 (1993).
- [19] The gradient  $\nabla u$  gives the local orientation of the chain relative to the x axis, while  $\nabla^2 u$  gives the local curvature of the chain. For small gradients,  $(\nabla u)^2/2$  describes the local contraction of the chain along its axis. As this "crumpling" occurs against the applied tension  $\tau$ , the second term gives the energy due to tension. Such a description is valid for a given chain segment for either a large bending stiffness or a sufficiently strong tension.
- [20] We note that for large  $\tau$ ,  $(L_{\infty} L)/L \sim kT \tan^{-1}(L/\pi\zeta)/\tau\zeta$ , where  $\zeta = \sqrt{\kappa/\tau}$ . This means that the tension diverges as  $\tau \sim 1/(L_{\infty} L)^2$  near full extension  $L \simeq L_{\infty}$ , in contrast with the behavior of freely jointed chains. This was recently pointed out for DNA by C. Bustamante, J. F. Marko, E. D. Siggia, and S. Smith, Science **265**, 1599 (1994). See also M. Fixman and J. Kovac, J. Chem. Phys. **58**, 1564 (1973).
- [21] R. H. Colby, M. Rubinstein, and J. L. Viovy, Macromolecules 25, 996 (1992).
- [22] C. F. Schmidt, M. Baermann, G. Isenberg, and E. Sackmann, Macromolecules 22, 3638 (1989).
- [23] Relative to the modulus of a flexible network,  $G' \sim kT\xi^{-3}$ , the moduli of Eqs. (6) and (8) are enhanced by  $(\ell_p/\xi)^2$  and  $(\ell_p/\xi)^{7/5}$ , respectively. Thus, for instance, for a network or gel with  $\xi=0.3~\mu\mathrm{m}$  and  $\ell_p \gtrsim 2.0~\mu\mathrm{m}$ , the modulus is enhanced by as much as 2 orders of magnitude.

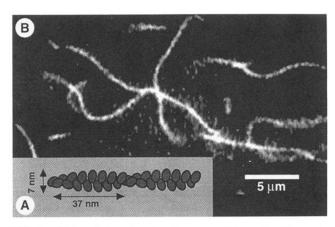


FIG. 1. Entangled network of semiflexible actin filaments. (A) In physiological conditions, individual monomeric actin proteins (G-actin) polymerize to form double-stranded helical filaments known as F-actin. These filaments exhibit a polydisperse length distribution of up to 70  $\mu$ m in length. The persistence length of these filaments is of order 2  $\mu$ m. (B) A dense solution (1.0 mg/ml) of actin filaments, approximately 0.03% of which have been labeled with rhodamine-phalloidin in order to visualize them by fluorescence microscopy. The average distance  $\xi$  between chains in this figure is approximately 0.3  $\mu$ m. Note the nearly straight conformation of the filaments on this scale.